
This copy is for your personal, non-commercial use only.

If you wish to distribute this article to others, you can order high-quality copies for your colleagues, clients, or customers by [clicking here](#).

Permission to republish or repurpose articles or portions of articles can be obtained by following the guidelines [here](#).

The following resources related to this article are available online at www.sciencemag.org (this information is current as of October 9, 2011):

Updated information and services, including high-resolution figures, can be found in the online version of this article at:

<http://www.sciencemag.org/content/333/6047/1262.full.html>

Supporting Online Material can be found at:

<http://www.sciencemag.org/content/suppl/2011/08/31/333.6047.1262.DC1.html>

A list of selected additional articles on the Science Web sites **related to this article** can be found at:

<http://www.sciencemag.org/content/333/6047/1262.full.html#related>

This article **cites 43 articles**, 15 of which can be accessed free:

<http://www.sciencemag.org/content/333/6047/1262.full.html#ref-list-1>

This article appears in the following **subject collections**:

Neuroscience

<http://www.sciencemag.org/cgi/collection/neuroscience>

A Gustotopic Map of Taste Qualities in the Mammalian Brain

Xiaoke Chen,¹ Mariano Gabitto,¹ Yueqing Peng,¹ Nicholas J. P. Ryba,² Charles S. Zuker^{1,3*}

The taste system is one of our fundamental senses, responsible for detecting and responding to sweet, bitter, umami, salty, and sour stimuli. In the tongue, the five basic tastes are mediated by separate classes of taste receptor cells each finely tuned to a single taste quality. We explored the logic of taste coding in the brain by examining how sweet, bitter, umami, and salty qualities are represented in the primary taste cortex of mice. We used *in vivo* two-photon calcium imaging to demonstrate topographic segregation in the functional architecture of the gustatory cortex. Each taste quality is represented in its own separate cortical field, revealing the existence of a gustotopic map in the brain. These results expose the basic logic for the central representation of taste.

The sense of taste is in charge of evaluating the nutritional value of a meal. In mammals, a very small palette of taste qualities orchestrates appetitive responses to energy- and protein-rich food sources (sweet and umami) and warns against the ingestion of toxic or spoiled/fermented foods (bitter and sour/carbonated). Salt sensing aids the adequate consumption of sodium while cautioning against the ingestion of excess salt. The attraction toward sweet, umami, and low-sodium, and the aversion toward bitter, sour, and high-salt, is innate and largely invariant throughout life. These observations suggest a physiological hard-wiring of tastant quality to hedonic value.

Each of the five basic tastes is detected by specialized sensors expressed on receptor cells of the tongue and palate epithelium (1–11). Over the past 10 years, we have shown that each receptor class is expressed in its own distinct taste cell type (2–6, 8, 12, 13). This “one cell, one taste” coding scheme is the hallmark of the organization of the mammalian taste system at the periphery, and is the mechanism through which individual taste qualities are recognized and encoded in the tongue (9, 14).

In rodents, information from taste cells in the oral cavity is transmitted to the primary taste cortex, the insula, through multiple neural stations (14, 15). How are the chemical senses represented in the cortex? Recent studies on the representation of odors in the primary olfactory cortex revealed a sparse and distributed pattern of neuronal activity whereby each odor is encoded by a unique ensemble of neurons, but without any spatial clustering or preference in relation to odorant space (16). This is in contrast to the organization of the primary visual, somatic, and auditory cortices, where neurons that

respond to similar features of the sensory stimulus are topographically organized into spatial maps in the cortex (17–19).

Previous studies examining how tastes are represented in the primary gustatory cortex have relied on a number of elegant approaches (20–25). Unfortunately, these experiments have led to inconclusive and often contradictory views of the central representation of taste, in part because of the limited spatial resolution of the techniques and/or the shortfalls of recording from small numbers of neurons (15, 26). We reasoned that if one could simultaneously examine the activity of large numbers of neurons in the insular cortex in response to taste stimulation (27), and do so with single-cell resolution, it should be possible to determine how the tastes are represented in the primary taste cortex.

Imaging gustatory responses in the primary taste cortex. We used two-photon calcium imaging (16, 28–30) to monitor tastant-evoked neural activity across the gustatory cortex *in vivo*. To confirm the appropriate region for imaging in mice (20, 25), we used extracellular electrodes to record tastant-evoked responses in the gustatory area of the thalamus (Fig. 1), and after identifying taste-responding cells, we used an AAV2/hu11-GFP virus (31) as an anterograde tracer to label (and trace) projections to the primary taste cortex (Fig. 1C) (32). These studies demarcated a domain of ~2.5 mm² in the insula, located ~1 mm above the intersection of the middle cerebral artery (MCA; Fig. 1, A and C) and the rhinal veins, and extending ~1 mm anteriorly, 1.5 mm posteriorly, and 1 mm dorsoventrally. Small areas of cortex were exposed in this region of the insula of anesthetized animals (via surgical craniotomy), and the neurons were bulk-loaded with the calcium-sensitive dye Oregon Green 488 BAPTA-1 AM (OGB) for functional imaging (Fig. 1D); this dye is effectively taken up by the cells (fig. S1) and serves as a robust fluorescent sensor of neural activity with high signal-to-noise ratios (16, 29, 30). To ensure that responses reflected biologically relevant stimuli, we used concentrations of tastants that reliably elicit ~80% of the maximal response in behavioral studies (3, 8).

Representation of bitter taste. We systematically inspected layer 2/3 of the gustatory cortex (a layer readily accessible by two-photon imaging) for tastant-evoked responses by parsing and tiling the insula into fields of 350 μm × 350 μm and testing for neurons that exhibited correlated patterns of tastant-dependent firing (16). The stimulus paradigm consisted of a pre-stimulus application of artificial saliva for 30 s, exposure to a test tastant for 10 s, and a post-stimulus artificial saliva wash for 30 s (32). We began by focusing on bitter taste, and discovered a highly localized, topographically defined cluster (i.e., a “hot spot” at ~1 mm dorsal to the rhinal veins and ~1 mm posterior to the MCA) (32), where many neurons responded to bitter stimuli with highly significant increases in intracellular calcium ($\Delta F/F$ ranging from 20 to 65%; Fig. 2); the location of the hot spot was stereotyped so that we could consistently find this cortical field in multiple animals (Fig. 2F and fig. S2). We examined the reproducibility of the taste-evoked responses in the hot spot by measuring variability across trials. We imaged ~200 neurons per trial, and these were segmented and coded according to their location and response magnitude (16, 33). On average, about one-third of the OGB-labeled neurons fired during the window of bitter tastant application, and the vast majority of these (>70%) responded in multiple bitter-stimulation trials (compare Fig. 2A and 2B; see also fig. S3). By examining bitter responses across the entire gustatory cortex in multiple animals, we confirmed this hot spot (i.e., cortical field) as the only region that exhibited correlated responses to bitter stimuli (Fig. 2F and fig. S2).

Are the bitter-responsive neurons selective or broadly tuned? We recorded from the bitter hot spot while stimulating the tongue with tastants representing the different taste qualities. Bitter-responding neurons were exquisitely tuned to bitter, with no other taste quality represented in this spatial domain of the gustatory cortex (Fig. 2). Equivalent results were obtained in single-unit electrophysiological recordings from within the bitter hot spot (fig. S4).

Humans and rodents recognize a wide range of bitter tasting chemicals, and their genomes correspondingly include a large number of genes that encode bitter taste receptors (T2Rs) (5–7). Most, if not all, T2Rs are expressed in the same subset of taste receptor cells (5), implying that these cells act as broadly tuned bitter sensors capable of detecting a wide range of bitter-tasting chemicals (5, 8). Thus, we predicted that the cortical representation for different bitter tastants should be shared. We therefore assayed the responses to several chemically distinct bitter tastants, and indeed all of them activated the same hot spot (Fig. 3 and fig. S3).

Specificity of cortical responses to taste stimuli. To further validate the specificity of the bitter cortical field, we examined taste responses in engineered mice where a single one of the

¹Howard Hughes Medical Institute, Department of Biochemistry and Molecular Biophysics, and Department of Neuroscience, College of Physicians and Surgeons, Columbia University, New York, NY 10032, USA. ²National Institute of Dental and Craniofacial Research, Bethesda, MD 20892, USA. ³Departments of Neurobiology and Neurosciences, University of California, La Jolla, CA 92093, USA.

*To whom correspondence should be addressed. E-mail: cz2195@columbia.edu

bitter taste receptors had been eliminated. T2R5 is one of the 36 bitter receptors in the mouse genome (34); it is necessary (and sufficient) for physiological and behavioral taste responses to the toxin cycloheximide, but not for detecting a wide range of other bitter chemicals (6, 8). If the bitter-evoked activity in the hot spot is indeed used to represent bitter taste, then all responses to cycloheximide should be missing in a T2R5 knockout (T2R5-KO) animal. However, responses to other bitter tastants should remain. This selective-loss experiment alleviates the uncertainty associated with examining animals with a total loss of bitter taste [e.g., TRPM5 or PLC β 2 knockouts (13)], as such a negative result could not be distinguished from a trivial failure to record cortical responses. As predicted, cycloheximide responses were abolished in the bitter hotspot of T2R5-KO animals, but responses to

other bitter chemicals were indistinguishable from those in control mice (Fig. 3).

A spatial map of taste qualities. Given the existence of a topographically defined region for the representation of bitter taste, we hypothesized that sweet taste would also be encoded in its own cortical field, and therefore surveyed the insular cortex for selective activity to sweet tastants. We discovered such a specific sweet hot spot at a considerable distance from the bitter hot spot (~2.5 mm rostradorsal to the bitter field; Fig. 4, A and B). There, a large ensemble of neurons responded to sweet taste stimulation of the tongue. Multiple lines of evidence validate that area as the sweet cortical field: First, the cells were preferentially tuned to sweet taste versus any of the other taste qualities (Fig. 4B and fig. S5). Second, the very same hot spot was activated by structurally different sweet-tasting chem-

icals (e.g., artificial versus natural sweeteners), but not by tastants for other taste qualities (Fig. 4, A and B, and fig. S5). Third, responses were abolished in sweet-receptor knockout animals [T1R2-KO (3); fig. S6]. Finally, this is the only region of gustatory insula that showed correlated activity in response to sweet taste.

The topographic separation of sweet and bitter taste into distinct and nonoverlapping gustatory fields in the primary taste cortex reveals the existence of a functional “gustotopic map.” In the other chemosensory modality, olfaction, individual odorants are represented in the primary olfactory cortex by the activation of spatially dispersed ensembles of neurons, without any discernible topographic or chemotopic organization (16). However, unlike the olfactory system—which must recognize, distinguish, and often initiate distinct physiological and behavioral responses to a vast universe of chemically distinct odorants—the chemical-perceptual space, represented by the five basic taste qualities, is remarkably limited (9, 14). Sweet and bitter exemplify the two poles of the gustatory spectrum; thus, we wondered whether the other taste qualities were also part of a gustatory map in the insula.

Umami is the savory taste that humans associate with monosodium glutamate (MSG); most other mammalian species use the umami-sensing taste receptor cells to recognize and mediate appetitive responses to protein-rich food sources [e.g., the taste of all amino acids (1, 2, 35)]. We searched the insular cortex for umami-evoked neuronal activity by stimulating the tongue with monopotassium glutamate (36). Indeed, just as seen for bitter and sweet, the cortical representation of umami was also part of the gustotopic map, with a unique hot spot for umami taste (Fig. 4, C and D, and fig. S5). The umami cortical field was specifically tuned to umami versus the other four taste qualities. As expected, this hot spot was activated by other L-amino acids (e.g., umami agonists; Fig. 4D) but not by their enantiomeric inactive D-forms (2, 3).

The remaining two basic tastes, salt (sodium) and sour (acid) sensing, are mediated by ion channel receptors rather than by G protein-coupled receptors (10–12, 37). Does the same organization apply to ionic tastes? Our efforts to uncover an acid (sour) hot spot did not succeed. We believe this could be because its location was outside the area sampled in our studies, or even because acid stimuli also act on a number of other pathways, such as pain and somatosensation (38), possibly leading to changes in its cortical representation. Thus, we focused on sodium taste.

Low concentrations of NaCl (i.e., appetitive salt taste) are sensed by a unique population of taste receptor cells via the ENaC ion channel (12). A salient feature of this response is its inhibition by amiloride and its strong selectivity for sodium versus other salts (12). Therefore, we searched for a salt-responsive cortical

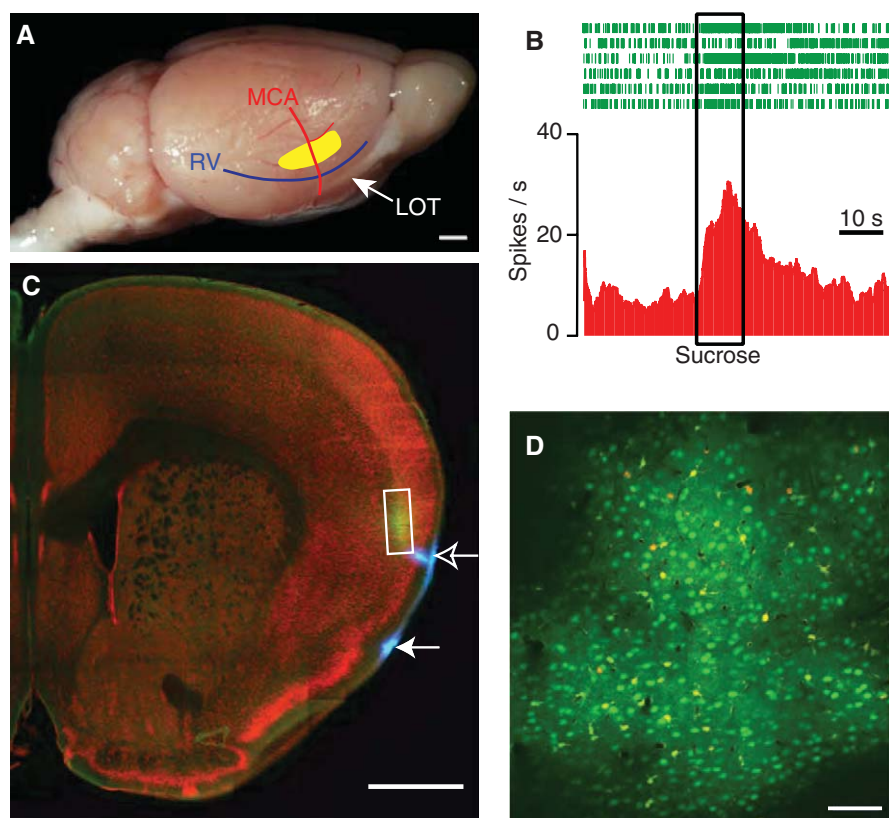


Fig. 1. Two-photon imaging in the mouse insular cortex. (A) Photograph of a mouse brain highlighting the approximate location of our imaging studies in the primary taste cortex (yellow). Also shown are the superimposed drawings of two key vascular landmarks (MCA, middle cerebral artery; RV, rhinal vein; LOT, lateral olfactory tract). (B) Responses of a sweet-sensitive thalamic taste neuron to 300 mM sucrose; the box indicates the time and duration of the sweet stimulus. After identification of such taste-responsive neurons, cells around the recording site were infected with an AAV2/hu11-GFP virus to label their terminal fields in layer 4 of the gustatory cortex. (C) Coronal section of a mouse brain (bregma +1.0) stained with TO-PRO-3 (red). Shown is the location of the thalamocortical projections labeled after infection with the AAV2/hu11-GFP virus (white box). To triangulate this region in relation to the vascular landmarks, we injected 1,1'-dioctadecyl-3,3,3',3'-tetramethylindocarbocyanine perchlorate (DiI) at the intersection between the RV and the MCA (pseudocolored in blue; solid arrow) and at 1 mm above (open arrow). (D) Images of bulk-loaded neurons and astrocytes in layer 2/3 of the primary gustatory cortex (see also fig. S1) stained with Oregon Green 488 BAPTA-1 AM (green fluorescence) and sulforhodamine 101 (yellow-labeled astrocytes). Animals were imaged using two-photon microscopy in vivo after surgical craniotomy. Scale bars, 1 mm [(A) and (C)], 100 μ m (D).

cluster that met those criteria. Just as shown for the other basic taste qualities, sodium taste is also represented in its own spatially segregated field (Fig. 4, E and F, and fig. S5). The responding neurons are exquisitely tuned to NaCl versus the other taste qualities, are sensitive to amiloride, and are specific for sodium versus other cations (e.g., KCl, MgCl₂).

Concluding remarks. For many years, the prevailing views about the organization and function of the taste system at the periphery centered around the concept of taste coding via broadly tuned taste receptor cells (39–41). Individual taste receptor cells were proposed to express receptors for various taste qualities and thus respond to multiple taste stimuli. Now, however, we know

that each of the five basic tastes is mediated by its own class of taste receptor cells, each tuned to a single taste quality, thus defining a “one cell, one taste” coding logic (9, 14). Notably, existing models of taste coding in the insula included proposals of broadly tuned neurons across taste qualities [with no spatial segregation (15)], as well as others suggesting a certain degree of topographic organization, but with no region dedicated to the processing of only one taste quality (20, 25, 26). Although we cannot rule out the existence of sparse numbers of broadly tuned cells (24, 26) distributed throughout the taste cortex (i.e., nonclustered), our results reveal that

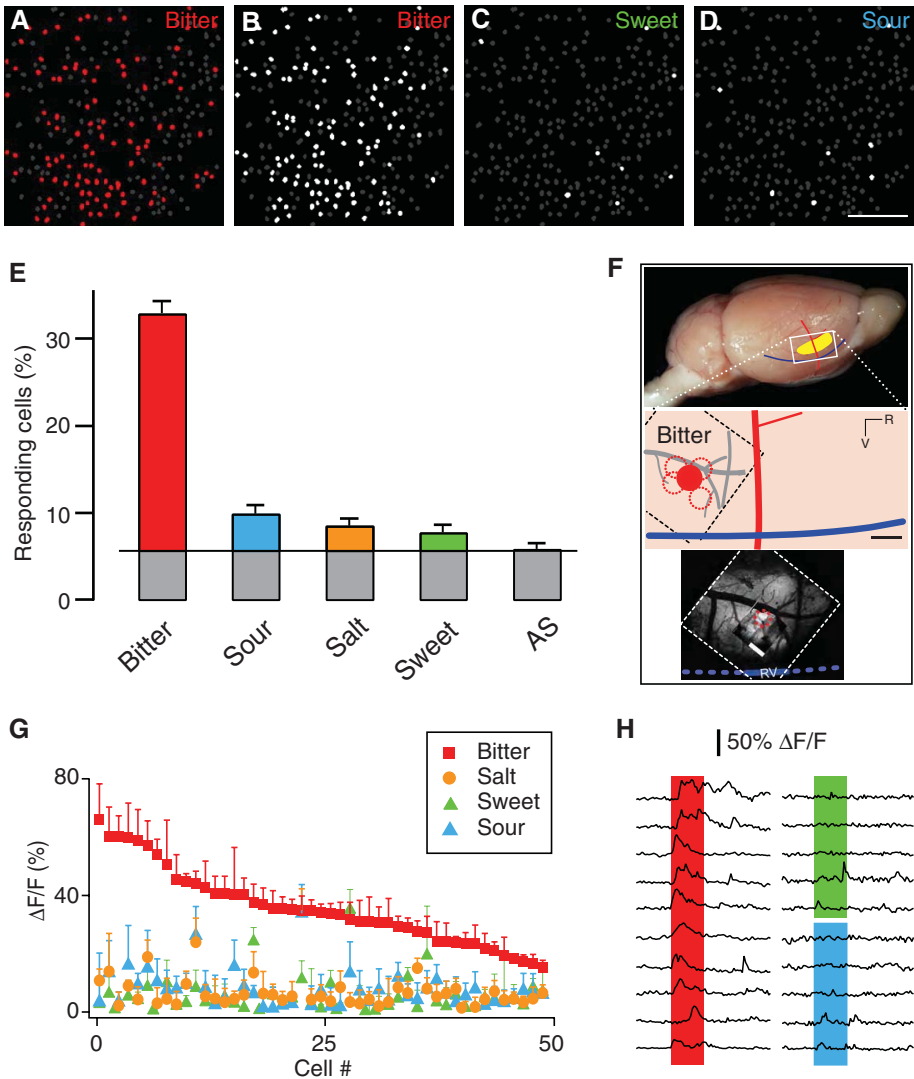


Fig. 2. Tastant-evoked responses in the bitter hot spot. (A) Bitter tastant stimulation of the tongue (single trial) evoked robust responses in the bitter hot spot. The image illustrates changes in OGB fluorescence in response to a 1 mM cycloheximide stimulus; ~35% of the loaded neurons responded with $\Delta F/F$ greater than 3.5 standard deviations above background (red cells; see also fig. S7). (B to D) In contrast to the sparse activity seen during application of other tastants [(C) and (D); see text], neurons activated by bitter tastant responded over multiple trials; cells that responded in at least two of four trials are labeled white (B). (E) Neurons in the bitter hot spot responded selectively to bitter versus other taste stimuli ($n = 8$). AS, artificial saliva. (F) An illustration and a bright-field image depicting the approximate relation of the bitter cortical field (solid red circle) to the vascular landmarks; the dotted circles depict the location of the bitter hot spot in four additional animals (32). The middle panel has been flattened to present a two-dimensional view of this area of the brain. (G) Bitter-responsive neurons are highly tuned to bitter taste (red). The graph shows the rank-ordered $\Delta F/F$ of a set of bitter-responsive neurons in a six-trial experiment to bitter stimuli versus other tastants (bitter = 1 mM cycloheximide; NaCl = 100 mM NaCl; sweet = 30 mM acesulfame K; sour = 10 mM citric acid). No apparent organization according to response amplitude was seen within the cluster (fig. S8). (H) Representative changes in OGB fluorescence during bitter (red), sweet (green), and sour (blue) stimulation for 10 s. Scale bars: 100 μ m [(A) to (D)], 0.5 mm (F); error bars are means \pm SEM.

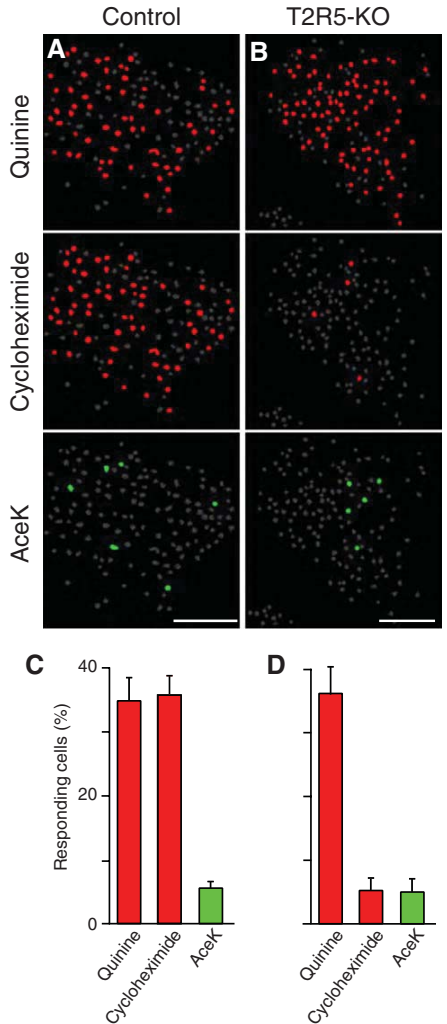


Fig. 3. Responses in the bitter hot spot are dependent on bitter taste receptor function. (A) Different bitter compounds activate the same hot spot in the cortex (see fig. S3) ($n = 4$). (B) Animals lacking the bitter taste receptor for cycloheximide (T2R5-KO) selectively lack cortical responses to cycloheximide but retain normal responses to other bitters (e.g., 10 mM quinine) ($n = 2$, seven trials per tastant). (C and D) Quantitation of taste responses in the control and T2R5-KO animals; also shown are data for a sweet tastant (acesulfame K). Note the lack of responses in both controls (C) and KO animals (D). Scale bars, 100 μ m; error bars are means \pm SEM.

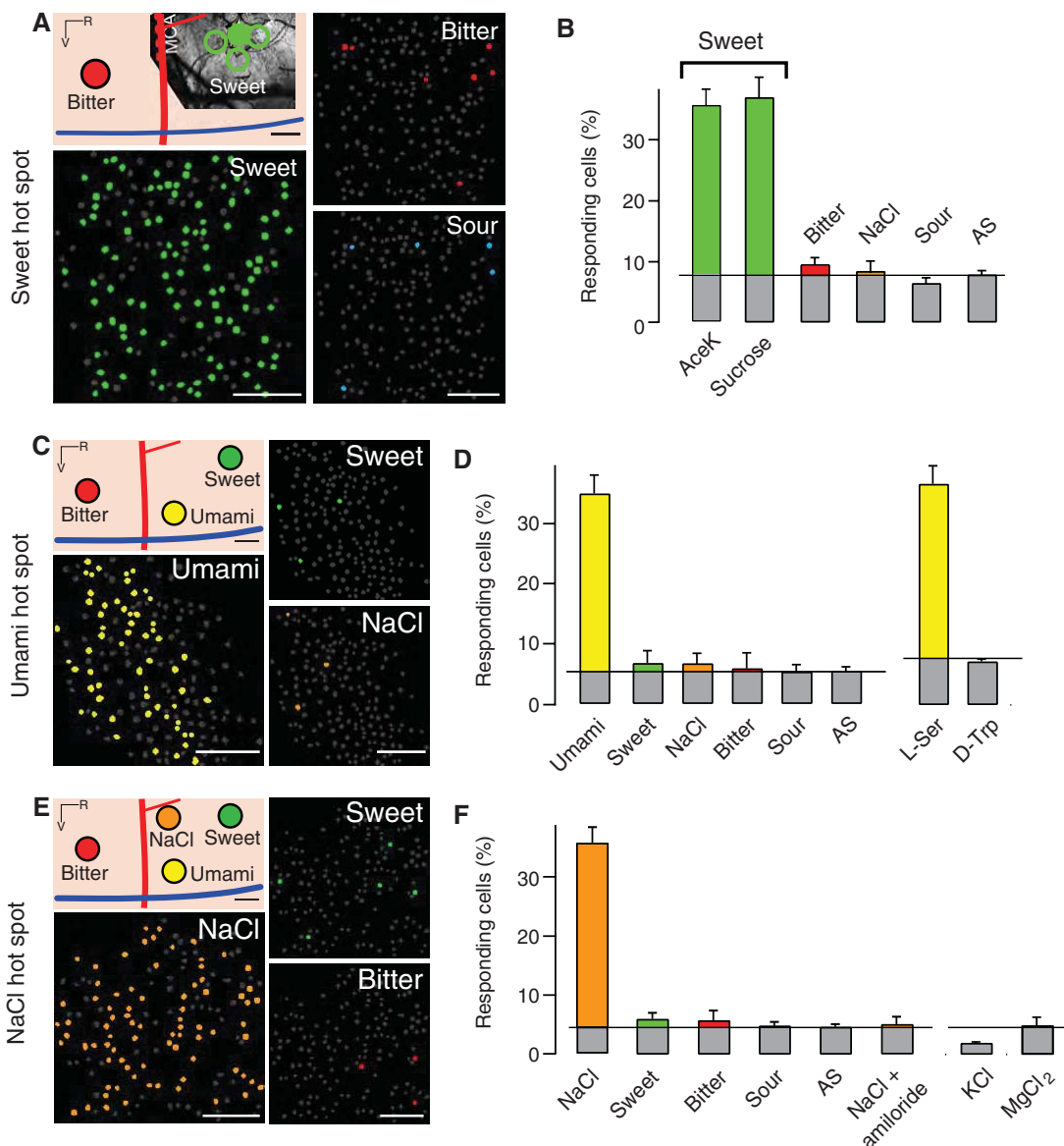
the individual basic tastes are represented in the insula by finely tuned cells organized in a precise and spatially ordered gustotopic map, where each taste quality is encoded in its own (segregated) stereotypical cortical field.

The organization of the primary taste cortex appears at first glance to be reminiscent of the somatosensory, auditory, and visual systems, which exhibit spatially organized somatotopic, tonotopic, and retinotopic cortical maps (17–19). However, the cortical maps for these three sensory modalities reflect smooth transitions across features of sensory space, whereas this is not the case in the taste system. Furthermore, in the somatosensory, auditory, and visual systems, the peripheral receptors display exacting spatial order,

whereas in taste, a distributed ensemble of peripheral receptor cells in the tongue—without any spatial organization, but with defined identities—nonetheless converge into a fixed cortical map where neurons with similar response profiles are clustered. Why should taste be represented in a spatial map? We speculate that this organization has an ancient evolutionary, possibly developmental, origin rather than a strictly functional origin. Indeed, the perceptual space to be represented by the taste system is limited to just a handful of qualities; thus, having each basic taste represented in individually segregated fields provides a simple and elegant architectural solution to pattern, wire, and interconnect the ensembles of neurons representing each taste quality.

Our studies suggest that the cortical fields representing the individual basic tastes cover only a small fraction of the insula. What does the rest of the insula do? We found that outside the hot spots, only small numbers of sparsely distributed neurons exhibited significant changes in fluorescence during the window of tastant presentation (fig. S6; see also fig. S4). The same results were observed in animals lacking taste receptor function (fig. S6) and irrespective of the quality of the taste stimulus (including artificial saliva alone); hence, these changes apparently do not represent responses to the individual basic tastes. Therefore, the inter-hot spot regions might be involved in other aspects of taste coding, such as the representation of taste mixes, and thus may

Fig. 4. The basic tastes are represented in a spatial map in the primary taste cortex. (A and B) Sweet taste is represented in its own cortical field (solid green circle), ~2.5 mm rostradorsal from the expected location of the bitter hot spot (red circle in upper left illustration). Also shown is the location of the sweet hot spot in three additional animals (open green circles). (A) About 35% of the OGB-labeled neurons in the sweet cortical field respond in multiple trials to sweet taste stimulation of the tongue (green-labeled neurons), but not to other tastes (e.g., bitter and sour). (B) The responses are highly specific for sweet tastants (see also fig. S7), including natural and artificial sweeteners. (C) Umami taste is also represented in its own stereotypical hot spot, found ~1 mm caudal and ventral to the expected sweet cortical field (yellow circle). (D) Responses are selective for umami tastants, including various L-amino acids, but not to D-amino acids or other taste qualities. (E) Low concentrations of sodium salt (100 mM NaCl) are known to activate a unique population of sodium-sensing taste receptor cells (12) and are represented in a distinct cortical field (orange circle) ~1 mm equidistant from the expected sweet and umami hot spots. (F) Amiloride completely abolishes both the function of the sodium taste receptor



and the insular representation of sodium taste. Other salts do not activate the sodium sensor (12) and indeed are not represented in the sodium hot spot (e.g., KCl, MgCl₂). See fig. S5 for additional details on the sweet, umami, and sodium responses. Scale bars, 100 μ m (0.5 mm in the cortex diagrams); error bars are means \pm SEM. The hot spots for the different

tastes are too far from each other to be imaged on the same animal; reconstructions are based on multiple animals. A minimum of four animals and four trials per animal/per tastant were used to define the sweet ($n = 10$ animals), umami ($n = 5$ animals), and sodium ($n = 4$ animals) cortical fields.

help to code the perception of “flavor” [e.g., responding to several tastes simultaneously (24, 26, 42)]. In addition, the insular cortex responds to more than just taste, and it is often thought of as a site for multisensory integration (15, 42, 43). Thus, these areas may participate in the integration of taste with the other senses.

The discovery of a gustotopic map in the mammalian cortex, together with the advent of sophisticated genetic and optical tools (44), should now make it possible to experimentally manipulate the taste cortex with exquisite finesse. In future studies, it will also be important to elucidate how taste intensity is encoded in the insular cortex, and to determine whether taste qualities with similar valence project to common targets. Likewise, tracing the connectivity of each of the basic taste qualities to higher brain stations will help decipher how these integrate with other modalities and combine with internal and emotional states to ultimately choreograph taste behaviors (45).

References and Notes

1. X. Li *et al.*, *Proc. Natl. Acad. Sci. U.S.A.* **99**, 4692 (2002).
2. G. Nelson *et al.*, *Nature* **416**, 199 (2002).
3. G. Q. Zhao *et al.*, *Cell* **115**, 255 (2003).
4. G. Nelson *et al.*, *Cell* **106**, 381 (2001).
5. E. Adler *et al.*, *Cell* **100**, 693 (2000).
6. J. Chandrashekar *et al.*, *Cell* **100**, 703 (2000).
7. H. Matsunami, J.-P. Montmayeur, L. B. Buck, *Nature* **404**, 601 (2000).
8. K. L. Mueller *et al.*, *Nature* **434**, 225 (2005).

9. J. Chandrashekar, M. A. Hoon, N. J. Ryba, C. S. Zuker, *Nature* **444**, 288 (2006).
10. A. L. Huang *et al.*, *Nature* **442**, 934 (2006).
11. Y. Ishimaru *et al.*, *Proc. Natl. Acad. Sci. U.S.A.* **103**, 12569 (2006).
12. J. Chandrashekar *et al.*, *Nature* **464**, 297 (2010).
13. Y. Zhang *et al.*, *Cell* **112**, 293 (2003).
14. D. A. Yarmolinsky, C. S. Zuker, N. J. Ryba, *Cell* **139**, 234 (2009).
15. S. A. Simon, I. E. de Araujo, R. Gutierrez, M. A. Nicolelis, *Nat. Rev. Neurosci.* **7**, 890 (2006).
16. D. D. Stettler, R. Axel, *Neuron* **63**, 854 (2009).
17. M. M. Merzenich, P. L. Knight, G. L. Roth, *J. Neurophysiol.* **38**, 231 (1975).
18. R. J. Tusa, L. A. Palmer, A. C. Rosenquist, *J. Comp. Neurol.* **177**, 213 (1978).
19. T. A. Woolsey, H. Van der Loos, *Brain Res.* **17**, 205 (1970).
20. R. Accolla, B. Bathellier, C. C. Petersen, A. Carleton, *J. Neurosci.* **27**, 1396 (2007).
21. H. Yoshimura, T. Sugai, M. Fukuda, N. Segami, N. Onoda, *Neuroreport* **15**, 17 (2004).
22. M. Sugita, Y. Shiba, *Science* **309**, 781 (2005).
23. E. S. Soares *et al.*, *Physiol. Behav.* **92**, 629 (2007).
24. J. R. Stapleton, M. L. Lavine, R. L. Wolpert, M. A. Nicolelis, S. A. Simon, *J. Neurosci.* **26**, 4126 (2006).
25. T. Yamamoto, *Prog. Neurobiol.* **23**, 273 (1984).
26. A. Carleton, R. Accolla, S. A. Simon, *Trends Neurosci.* **33**, 326 (2010).
27. D. B. Katz *et al.*, *J. Neurosci.* **28**, 11802 (2008).
28. J. N. Kerr *et al.*, *J. Neurosci.* **27**, 13316 (2007).
29. K. Ohki, S. Chung, Y. H. Ch'ng, P. Kara, R. C. Reid, *Nature* **433**, 597 (2005).
30. C. Stosiek, O. Garaschuk, K. Holthoff, A. Konnerth, *Proc. Natl. Acad. Sci. U.S.A.* **100**, 7319 (2003).
31. C. N. Cearley *et al.*, *Mol. Ther.* **16**, 1710 (2008).
32. See supporting material on Science Online.
33. T. Komiyama *et al.*, *Nature* **464**, 1182 (2010).
34. S. V. Wu, M. C. Chen, E. Rozengurt, *Physiol. Genomics* **22**, 139 (2005).

35. K. Iwasaki, T. Kasahara, M. Sato, *Physiol. Behav.* **34**, 531 (1985).
36. We used the monopotassium form of glutamate to prevent confounding activity from a potential sodium taste hot spot (3).
37. S. C. Kinnamon, R. F. Margolskee, *Curr. Opin. Neurobiol.* **6**, 506 (1996).
38. T. Arai, T. Ohkuri, K. Yasumatsu, T. Kaga, Y. Ninomiya, *Neuroscience* **165**, 1476 (2010).
39. A. Caicedo, K. N. Kim, S. D. Roper, *J. Physiol.* **544**, 501 (2002).
40. T. A. Gilbertson, J. D. Boughter Jr., H. Zhang, D. V. Smith, *J. Neurosci.* **21**, 4931 (2001).
41. T. Sato, L. M. Beidler, *Chem. Senses* **22**, 287 (1997).
42. D. B. Katz, S. A. Simon, M. A. Nicolelis, *J. Neurosci.* **21**, 4478 (2001).
43. M. Kadohisa, E. T. Rolls, J. V. Verhagen, *Chem. Senses* **30**, 401 (2005).
44. L. Fennó, O. Yizhar, K. Deisseroth, *Annu. Rev. Neurosci.* **34**, 389 (2011).
45. A. Fontanini, D. B. Katz, *Ann. N.Y. Acad. Sci.* **1170**, 403 (2009).

Acknowledgments: We thank A. Devor and Y. Dan for their hospitality and technical help with our early intrinsic imaging attempts, R. Barreto for valuable help with imaging and data analysis, S. Hunter-Smith for help with viral tracing experiments, and R. Axel, K. Scott, D. Steddler, R. Bruno, and members of the Zuker lab for helpful comments. Supported by a Human Frontier Science Program fellowship (X.C.) and by the Intramural Research Program of the National Institute of Dental and Craniofacial Research. C.S.Z. is an investigator of the Howard Hughes Medical Institute.

Supporting Online Material

www.sciencemag.org/cgi/content/full/333/6047/1262/DC1

Materials and Methods

Figs. S1 to S8

References

9 February 2011; accepted 8 July 2011

10.1126/science.1204076

REPORTS

Vacuum-Induced Transparency

Haruka Tanji-Suzuki,^{1,2*} Wenlan Chen,² Renate Landig,² Jonathan Simon,¹ Vladan Vuletić²

Photons are excellent information carriers but normally pass through each other without consequence. Engineered interactions between photons would enable applications as varied as quantum information processing and simulation of condensed matter systems. Using an ensemble of cold atoms strongly coupled to an optical cavity, we found that the transmission of light through a medium may be controlled with few photons and even by the electromagnetic vacuum field. The vacuum induces a group delay of 25 nanoseconds on the input optical pulse, corresponding to a light velocity of 1600 meters per second, and a transparency of 40% that increases to 80% when the cavity is filled with 10 photons. This strongly nonlinear effect provides prospects for advanced quantum devices such as photon number–state filters.

The experimental realization of strong coherent interactions between individual photons will enable a variety of applications such as quantum computing (1–3) and studies of strongly correlated many-body quantum systems (4). Two main approaches to generating photon-photon interactions are strong coupling of single emitters to optical cavities

(2, 3, 5–9) and electromagnetically induced transparency (EIT) in ensembles of atoms (10–12). Single emitters strongly coupled to cavities can provide substantial optical nonlinearity at the expense of typically large input-output coupling losses and the technical challenges of trapping and manipulating single particles. EIT in atomic ensembles provides an impressive degree of coherent control in simple, elegant experiments (12–15), but the nonlinearities achieved so far are relatively weak, requiring (for example) ~500 photons for all-optical switching (16). We demonstrate that by using an optical cavity to enhance the EIT control field, the resonant transmission

of light through an atomic ensemble can be substantially altered by a few photons and even by the cavity vacuum (17, 18). Because the effect is nonlinear in both control and probe fields at the single-photon level, it should enable advanced quantum optical devices such as photon number–state filters (19) and nondestructive photon number–resolving detectors (20, 21). We call the limiting case with no photons initially in the cavity “vacuum-induced transparency” (VIT) (17) to distinguish it from recent cavity EIT demonstrations using a single atom with cavity-enhanced absorption and a classical control field containing many photons (22, 23). In contrast, VIT may be realized with only one photon in the entire system.

We experimentally realize Field’s original proposal (17) to replace the EIT control field by the vacuum field inside a strongly coupled cavity (Fig. 1). In an atomic Λ system $|f\rangle \leftrightarrow |e\rangle \leftrightarrow |g\rangle$ with two stable states $|f\rangle$, $|g\rangle$, the probe beam addresses the $|f\rangle \rightarrow |e\rangle$ transition, whereas the cavity mode is tuned near the $|g\rangle \rightarrow |e\rangle$ transition. A cold atomic ensemble is prepared in the state $|f\rangle$ by optical pumping. VIT for the probe beam can be thought of as arising from a vacuum-induced Raman process where the incoming probe photon is absorbed, quickly emitted into the cavity, then reabsorbed by the ensemble and reemitted

¹Department of Physics, Harvard University, Cambridge, MA 02138, USA. ²Department of Physics, MIT-Harvard Center for Ultracold Atoms, and Research Laboratory of Electronics, Massachusetts Institute of Technology, Cambridge, MA 02139, USA.

*To whom correspondence should be addressed. E-mail: haruka.tanji@post.harvard.edu